(12) NACH DEM VERTRAG ÜBER DIE INTERNATIONALE ZUSAMMENARBEIT AUF DEM GEBIET DES PATENTWESENS (PCT) VERÖFFENTLICHTE INTERNATIONALE ANMELDUNG

BERICHTIGTE FASSUNG

(19) Weltorganisation für geistiges Eigentum
Internationales Büro

(43) Internationales Veröffentlichungsdatum
8. Januar 2004 (08.01.2004)

PCT

(10) Internationale Veröffentlichungsnummer
WO 2004/003063 A1

(51) Internationale Patentklassifikation[7]: C08J 9/00, 9/12

(21) Internationales Aktenzeichen: PCT/EP2003/006941

(22) Internationales Anmeldedatum:
30. Juni 2003 (30.06.2003)

(25) Einreichungssprache: Deutsch

(26) Veröffentlichungssprache: Deutsch

(30) Angaben zur Priorität:
102 29 983.8 3. Juli 2002 (03.07.2002) DE

(71) Anmelder *(für alle Bestimmungsstaaten mit Ausnahme von US)*: FAGERDALA DEUTSCHLAND GMBH [DE/DE]; Herrenhöfer Landstrasse 6, 99885 Ohrdruf (DE).

(72) Erfinder; und

(75) Erfinder/Anmelder *(nur für US)*: ZIEGLER, Maik [DE/DE]; Wiesenstrasse 7, 99887 Gräfenhain (DE).

(74) Anwalt: BUNKE, Holger; Prinz & Partner GbR, Manzingerweg 7, 81241 München (DE).

(81) Bestimmungsstaaten *(national)*: AE, AG, AL, AM, AT, AU, AZ, BA, BB, BG, BR, BY, BZ, CA, CH, CN, CO, CR, CU, CZ, DE, DK, DM, DZ, EC, EE, ES, FI, GB, GD, GE, GH, GM, HR, HU, ID, IL, IN, IS, JP, KE, KG, KP, KR, KZ, LC, LK, LR, LS, LT, LU, LV, MA, MD, MG, MK, MN, MW, MX, MZ, NO, NZ, OM, PH, PL, PT, RO, RU, SC, SD, SE, SG, SK, SL, TJ, TM, TN, TR, TT, TZ, UA, UG, US, UZ, VC, VN, YU, ZA, ZM, ZW.

(84) Bestimmungsstaaten *(regional)*: ARIPO Patent (GH, GM, KE, LS, MW, MZ, SD, SL, SZ, TZ, UG, ZM, ZW), eurasisches Patent (AM, AZ, BY, KG, KZ, MD, RU, TJ, TM), europäisches Patent (AT, BE, BG, CH, CY, CZ, DE, DK, EE, ES, FI, FR, GB, GR, HU, IE, IT, LU, MC, NL, PT, RO, SE, SI, SK, TR), OAPI Patent (BF, BJ, CF, CG, CI, CM, GA, GN, GQ, GW, ML, MR, NE, SN, TD, TG).

Veröffentlicht:
— *mit internationalem Recherchenbericht*

(48) Datum der Veröffentlichung dieser berichtigten Fassung: 22. Juli 2004

(15) Informationen zur Berichtigung:
siehe PCT Gazette Nr. 30/2004 vom 22. Juli 2004, Section II

Zur Erklärung der Zweibuchstaben-Codes und der anderen Abkürzungen wird auf die Erklärungen ("Guidance Notes on Codes and Abbreviations") am Anfang jeder regulären Ausgabe der PCT-Gazette verwiesen.

(54) Title: THERMOPLASTIC FOAMED MATERIALS COMPRISING NANOSTRUCTURED FILLING MATERIALS AND METHOD FOR PRODUCING THE SAME

(54) Bezeichnung: THERMOPLASTISCHE SCHAUMSTOFFE MIT NANOSTRUKTURIERTEN FÜLLSTOFFEN UND VERFAHREN ZU IHRER HERSTELLUNG

(57) Abstract: The invention relates to physically expanded thermoplastic foamed materials consisting of a polymer matrix and fine-particle filling materials which are incorporated into the polymer matrix, and having a density of between 8 and 350 g/l. Said foamed materials contain between 0.001 and 40 mass % of nanoparticles as filling materials. The invention also relates to a method for producing foamed materials, whereby a thermoplastic polymer in the form of a granulated material is supplied to an extruder, along with fine-particle filling materials, and is extruded to form a polymer compound. Said compound is expanded by means of a physical blowing agent, either simultaneously or subsequently, and is extruded to form foamed particles, a foamed plate or a foamed film. Nanoparticles are used as filling materials in a quantity of between 0.001 and 40 mass %.

(57) Zusammenfassung: Die Erfindung betrifft physikalisch expandierte thermoplastische Schaumstoffe aus einer Polymermatrix und darin eingelagerten feinteiligen Füllstoffen und mit einer Dichte zwischen 8 und 350 g/l, die 0,001 - 40 Masseprozent Nanopartikel als Füllstoffe enthalten. Die Erfindung betrifft ferner ein Verfahren zur Herstellung der Schaumstoffe, bei dem ein thermoplastisches Polymer in Form eines Granulats zusammen mit feinteiligen Füllstoffen einem Extruder zugeführt und zu einem Polymer-Compound extrudiert werden, wobei das Compound gleichzeitig oder danach mittels physikalischer Treibmittel aufgeschäumt und zu Schaumpartikeln, einer Schaumplatte oder einer Schaumfolie extrudiert wird, wobei als Füllstoffe wiederum Nanopartikel in einer Menge von 0,001 - 40 Masseprozent verwendet werden.

WO 2004/003063 A1

POLYMER/CLAY NANOCOMPOSITE FOAMS PREPARED BY CO_2

Changchun Zeng, Yong Yang, Xiangmin Han, L. James Lee and D. L. Tomasko
Department of Chemical Engineering
The Ohio State University
Columbus, OH 43210

Abstract

Polymeric foams are widely used in many applications. In this study, we prepared polymer/clay nanocomposite foams using carbon dioxide as the foaming agent. The effect of clay dispersion (intercalation vs. exfoliation), clay concentration and types of polymers on foam morphology were investigated. It was found that clay nanoparticles serve as an efficient nucleation agent. The nucleation efficiency is affected by both clay dispersion and polymer-clay-CO_2 interaction. By controlling nanocomposite composition and foaming conditions, PMMA nanocomposite foams with cell size as small as ~0.4 μm and cell density as high as ~10^{12} cells/cc can be produced. These foams exhibit good combination of stiffness, toughness, weight saving and dimension stability. In addition, PLGA nanocomposites foams were also prepared and they can be used for tissue engineering scaffolds.

Introduction

Polymer based foams are widely used in many applications, from packaging materials, insulation panels, cushions, to scaffolds for tissue engineering. Recently developed microcellular foams have drawn a great deal of attention and interest. These microcelluar foams have pore size less than 10 microns and foam density about 0.5 to 0.8 g/cc. They have good properties [1].

To obtain cells with controlled structure and distribution, a common practice is to add particles (nucleation agents) to reduce the nucleation energy. The presence of filler also promotes the accumulation of gas on the polymer-particle interface and creation of nucleation sites [2]. Generally, the particles used in these studies are of micron size. Two key factors that determine the foam quality when applying particles to assist nucleation are the amount and distribution of the nucleation agents. A nonuniform distribution of the agents may result in a foam that has a high concentration of gas bubbles or cells in the agent rich area and a low concentration in agent poor areas. Thus the uniformity of the cell structure and the cell density are limited by the method used to mixed agents and the polymer. In fact, it is rather hard to obtain a uniform cell structure with a high cell density in the conventional foaming process using microparticles [3].

We have reported the use of clay nanoparticles to control polystyrene (PS) foam morphology, leading to improved mechanical properties and fire resistance of the foam materials [4, 5]. By controlling surface chemistry and processing conditions, clay nanoparticles can be uniformly dispersed in the PS matrix. Thus a low nominal particle concentration can provide large number of sites for nucleation.

In this study, we extend our work on polymer clay nanocomposites foams to other types of polymers. We synthesized a series of poly(methyl methacrylate) (PMMA) and poly(lactide-glycolide) (PLGA) nanocomposites either by extrusion compounding or in-situ polymerization. These nanocomposites were then foamed via a batch foaming processing using supercritical carbon dioxide as the foaming agent. The effects of clay on the cell morphology are investigated.

Experimental

Materials

Methylmethacrylate (MMA) and initiator 2,2'-azobisisobutyronitrile (AIBN) were purchased from Aldrich. A PMMA resin (PL25 from Plaskolite) was used to prepare nanocomposites by extrusion. PLGA (5050 High IV) was kindly supplied by Alkermes. Three types of organically modified montmorillonite clays were used in this study. Cloisite 20A (20A) and 30B (30B) were donated by Southern Clay. Clay was prepared MHABS is in-house [6]. The chemical structures of the surfactants in the organically modified clays are shown in Figure 1. The foaming agent, a bone-dry grade carbon dioxide, was provided by Praxair.

Preparation of Polymer/Clay Nanocomposites

Both twin-screw extrusion and in-situ polymerization were used to prepare PMMA/clay nanocomposites. In-situ polymerization was carried out under isothermal conditions at 50°C. The monomer, clay and AIBN (0.5wt%) were mixed together using a high shear mixer. The mixture was reacted at 50°C for 20 hrs, then the temperature was raised to 105°C for another 30 min. Intercalated PMMA/20A nanocomposites were prepared using a Leistritz ZSE-27 fully intermeshing twin-screw extruder (L/D= 40, d= 27 mm) operated in the co-rotating mode. The screw speed was 200 rpm. The extruder temperature was 200°C. PLGA/30B

nanocomposite was prepared via solvent casting. PLGA and clay were placed in acetone and sonicated for 3 hours. Solvent was then evaporated after which the nanocomposite was dried in vacuum oven.

Foaming of Nanocomposites

Batch foaming was performed under constant pressure and temperature. Stainless steel tubing was used as the pressure vessel. CO_2 was delivered via a syringe pump. The system was allowed to equilibrate for 24 hours for CO_2 to reach saturation in the polymer matrix. The pressure was then rapidly released and the foamed cells were fixed with or without the use of cooling water depending on the foaming temperatures. A two-step foaming process was also used. In this process, polymers and their nanocomposites were saturated with CO_2 at a temperature well below their normal glass transition temperatures. They were subsequently taken out and placed in a hot water batch for certain period of time, after which they were quenched in ice water. The reduced CO_2 solubility in polymer matrix lead to the nucleation and expansion of gas bubbles.

Analytical Methods

The X-ray diffraction (XRD) patterns of prepared polymer/clay nanocomposites were recorded on a Scintag XDS-2000 X-ray diffractometer with Cu Kα radiation and operated at 35kV and 10mA. A Phillip XL30 scanning electron microscope was also used to observe the cell morphology.

Results and Discussion

Structure of Nanocomposites

Montmorillonite clay particles contain many crystallites (tactoids) which in turn are composed of a large number of platelets-like individual layers with a thickness dimension ~1 nm and lateral dimension of from several hundred nanometers up to ~1μm. Formation of nanocomposites relies on polymer chain penetration and interlayer expansion, depending on the compatibility of the polymer matrix and the clay surface [7, 8]. Complete disruption and delamination of the tactoids lead to the formation of exfoliated nanocomposites, in which the clay layers have been substantially separated and dispersed in the polymer matrix. On the other hand, limited compatibility of polymers and clay surface results in limited polymer penetration into the clay gallery and intercalated nanocomposites. The structure registry in the layered structure remains and is detectable by x-ray diffraction (XRD). Figure 2 shows the XRD of PMMA/clay nanocomposites. The diffraction pattern of 20A is included as a reference. PMMA/5%20A has a distinct diffraction peak, with a basal spacing of 3.6 nm. Comparing to the basal spacing of 20A (2.3 nm), PMMA intercalation is evident. On the other hand, the PMMA/5%MHABS nanocomposites does not show any diffraction peak, indicating clay tactoids have been delaminated and an exfoliated nanocomposite is achieved. Figure 3 shows the diffraction pattern of clay 30B as well as PLGA/5%30B nanocomposites. After intercalation, the basal spacing expands from 1.8 nm to 3.3 nm.

Effect of Clay on Foam Structure

Batch foaming were conducted to compare the effect of different clay dispersions on cell morphology of PMMA and PMMA nanocomposites foams. As shown in Figure 4. the addition of 5wt% of clay causes a decrease in cell size decreases and an increase in cell density. Image analysis was used to obtain the average cell size and cell density. In the presence of 5%20A, the cell size decreases from 8.2μm to 5.4μm, and the cell density increases from 1.62×10^9 cells/cc to 4.22×0^9 cells/cc. The exfoliated nanocomposite foam has a much smaller cell size and much higher cell density. The average cell size is around 1.6μm and cell density around 1.51×10^{11} cells/cc. Addition of clay greatly influences cell size and cell density of PMMA foams. This trend is similar to our previous study of PS/clay nanocomposites foams [4, 5]. Clay may serve as a heterogeneous nucleation agent allowing more sites to nucleate. This leads to an increase in cell density and decrease in cell size under the same foaming conditions. Classical nucleation theory can qualitatively explain the effect of clay dispersion on the nucleation rate [9]. In the case of heterogeneous nucleation where particles are added, the nucleation rate is given by $N_{het} = f_1 C_1 \exp(-\Delta G^*_{het}/kT)$, where f_1 is the frequency factor representing the frequency that gas molecules joining the embryo of a nucleus. C_1 is the concentration of heterogeneous nucleation sites, which is directly related to the particle concentration. ΔG^*_{het} is the Gibbs free energy for heterogeneous nucleation, which is given by $\Delta G^*_{het} = 16\pi\gamma^3_{bp} f(\theta)/3(\Delta P)^2$, where $f(\theta) = (1/4)(2+\cos\theta)(1-\cos\theta)^2$, θ is the contact angle at the gas-particle-polymer interface. In intercalated nanocomposites, most clay exists as stacks of layers or tactoids, serving as nucleation sites. On the other hand, in exfoliated nanocomposites, clay is present mostly as individual layers or stacks of a few layers. Usually the distance between the layers is greater than the effective radius of gyration of a polymer chain. Much more clay platelets are in direct contact with the matrix, providing much larger interfacial area for CO_2 adsorption and cell nucleation. Thus C_1 is much higher, resulting in a higher nucleation rate and ultimately higher a cell density.

However, a significant difference of effect of clay MHABS on the cell density of PMMA and PS is observed and can not be explained by the increase of nucleation

sites alone. Table 1 is a summary of normalized cell density of PMMA and PS nanocomposite foams. The PS nanocomposites foam data were taken from reference [4]. Five percent 20A has a similar effect on cell density increase for both PMMA and PS (2.6 for PMMA vs. 1.6 for PS). However, the increase of cell density is significantly higher for PMMA than for PS when 5% MHABS is present. The former has a cell density more than 90 times higher than pure PMMA foam, while the latter only shows about five fold increase in cell density compared to the pure PS foam.

The difference of MHABS dispersion in these two matrices is not expected to cause the drastic difference in cell morphology, as MHABS is well dispersed in both matrices. Here we propose a possible mechanism based on the interaction of polymer-CO_2-particles. Both nanocomposites were prepared via in-situ polymerization and rely on the interlayer copolymerization of MHAB with monomer to achieve exfoliation. The growing polymer is expected to cover the clay surface. The main difference between the copolymers coated on clay surface in PMMA/MHABS and that in PS/MHABS nanocomposites is shown in Figure 5. In PMMA/MHABS, the copolymer is essentially PMMA with a cationic ammonium head group bonded to the clay surface. On the other hand, the copolymer in PS/MHABS is a PS polymer containing one methacrylic group. This is important in that the former has a much higher affinity to CO_2 due to a large number of carbonyl group. More CO_2 is likely to be attracted on to the surface to form nucleus. Furthermore, a strong affinity between CO_2 and the carbonyl group of the copolymers coated on the clay surface in the PMMA/MHABS system may improve surface wetting and consequently reduce the contact angle. These two factors may contribute to a higher nucleation rate. Considering the strong dependence of Gibbs free energy on the contact angle, it is not surprising to see a significantly different nucleation rate between these two systems. Further investigation is being carried out to verify this hypothesis in our laboratory. Nevertheless, by deliberate surface modification of clay, it is possible to improve not only clay dispersion and consequently the number of nucleation sites, but also the interaction between polymer-CO_2-particle surfaces for enhanced nucleation efficiency.

Effect of Foaming conditions

In classical nucleation theory, the available amount of gas molecules directly contributes to the number of nuclei formed and thus the cell density [9]. Bubble growth also relies on gas diffusion from the polymer-gas solution into the forming bubbles. A higher gas concentration will therefore be beneficial in increasing the cell density in polymeric foams. Recent studies [10] have shown that under a low temperature and moderate pressure, CO_2 has an unusually higher solubility in PMMA. It is reported that PMMA microcellular foams with submicron cell size can be produced without using very high pressure [10, 11]. By combing high CO_2 solubility and the nucleation effect of clay, it is possible to produce foams with even higher cell density and smaller cell size. Thus PMMA and its nanocomposites were foamed using a two step process. First, the materials were placed in a pressurized vessel and saturated with CO_2 at 3.45×10^6 Pa (500 psi) and 0°C for sufficiently long time to ensure equilibrium. The vessel was then placed in hot water batch at 80°C, after which it was quenched using ice water mixture. Figure 6 shows the SEM micrograph of PMMA and the PMMA nanocomposite foams where foaming time is 15 seconds. The pure PMMA foam shows open-cell morphology, while both intercalated and exfoliated nanocomposite foams exhibit closed-cell morphology. The intercalated PMMA/20A nanocomposite foam exhibits a bimodal cell size distribution. The larger bubbles are probably formed around big clay tactoids, while smaller bubbles may form around small clay tactoids. On the other hand, the exfoliated PMMA/MHABS nanocomposite foam shows much higher cell density and smaller cell size than the intercalated PMMA/20A nanocomposite foam. Image analysis reveals that the average cell size of PMMA/MHABS nanocomposites foam is around 0.37 um and cell density around 1.86×10^{12} cells/cc. Preliminary testing showed that these foams provided good balance of stiffness and toughness. Detailed characterization of mechanical properties and dielectric properties are underway in our laboratory.

PLGA Nanocomposite Foam

PLGA is a biodegradable polymer and PLGA foam is commonly used as three dimensional scaffold materials for cell attachment and growth in biological applications [12]. Conventional foam materials have nonuniform cell size distribution, making them less than ideal. Microfabrication has been adopted to create well-defined two-dimensional structure. By using CO_2 assisted bonding, layers of well-defined 2D structures can be bonded together to create 3D scaffold [13]. A critical aspect in creating scaffold using this approach is to generate open foam cells on the 2D structures during bonding, to ensure nutrient transfer within as well as between the 2D structures. In this study, PLGA/30B nanocomposite was used to create desired foam morphology. The nanocomposites was saturated at 35°C and foamed at 1.03×10^6 Pa (150 psi). Figure 7 is an SEM micrograph of the bonded region of the 3D scaffold material. A large number of very small pores was generated and they exhibit some degree of openess. The overall dimension of the scaffold is well preserved. This preliminary result shows the feasibility of creating connected pores between the 2D structure. We are currently continuing the investigation of the foaming and bonding mechanism of PLGA/clay nanocomposites in pressured CO_2 to make a suitable scaffold.

Summary

Several types of polymer/clay nanocomposites foams have been prepared using CO_2 as the foaming agent. It is found that clay is an effective nucleation agent. The nucleation efficiency is affected by both clay dispersion and polymer-clay-CO_2 interaction. Microcellular PMMA nanocomposite foams with exceptionally high cell density and small cell size can be produced under mild conditions. PLGA nanocomposite foams were also prepared. They exhibit open pore structure and has the potential to be used as tissue engineering scaffolds.

References

1 Kumar, V. and Weller, J. E., *ACS Symp. Ser.*, **669**, 101 (1997).

2 Chen, L., Straff, R. and Wang, X., *ANTEC SPE*, **2**, 1732 (2001).

3 Lee, S.-T., *Foam Extrusion: Principles and Practice*. Lancaster, PA: Technomic Publishing Company, Inc. 2000.

4 Zeng, C., Han, X., Lee, L. J., Koelling, K. W. and Tomasko, D. L., *ANTEC SPE*, **2**, 1504 (2002).

5 Han, X., Zeng, C., Lee, L. J., Koelling, K. W. and Tomasko, D. L., *ANTEC SPE*, **2**, 1915 (2002).

6 Zeng, C., Han, X., Lee, L. J., Koelling, K. W. and Tomasko, D. L., (Manuscript in preparation).

7 Vaia, R. A. and Giannelis, E. P., *Macromolecules*, **30**, 8000 (1997).

8 Vaia, R. A. and Giannelis, E. P., *Macromolecules*, **30**, 7990 (1997).

9 Colton, J. S. and Suh, N. P., *Polym. Eng. Sci.*, **27**, 485 (1987).

10 Handa, P. Y., Zhang, Z. and Wong, B., *Cellular Polymers*, **20**, 1 (2001).

11 Handa, P. Y. and Zhang, Z., *Journal of Polymer Science: Part B: Polymer Physics*, **38**, 716 (2000).

12 Sparacio, D., Beckman, E. J. *ACS Symp. Ser.*, **713**, 181 (1998).

13 Yang, Y., Han, X., Zeng, C., Lee, L. J. and Tomasko, D. L., AIChE Annual Meeting, Indianapolis (2002).

Table 1 Comparison of cell density

PMMA series	normalized cell density	PS seires	normalized cell density
PMMA	1.0	PS	1.0
5%20A	2.6	5%20A	1.6
5%MHABS	93.5	5%MHABS	4.9

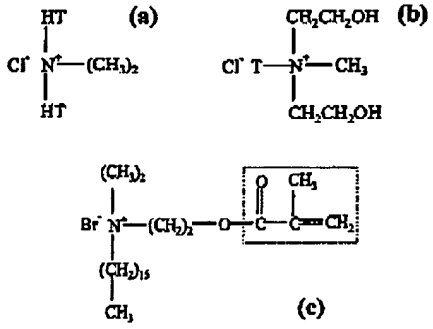

Figure 1 Chemical structures of surfactants in (a) 20A; (b) 30B; (c) MHABS. T represents tallow (C_{18}~65%, C_{16}~30%, C_{14}~5%), HT is hydrogenated tallow.

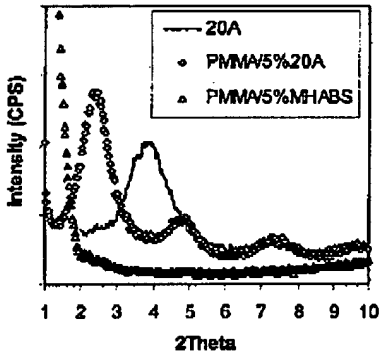

Figure 2 XRD of PMMA nanocomposites.

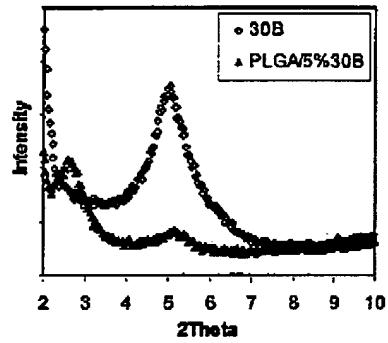

Figure 3 XRD of PLGA nanocomposite.

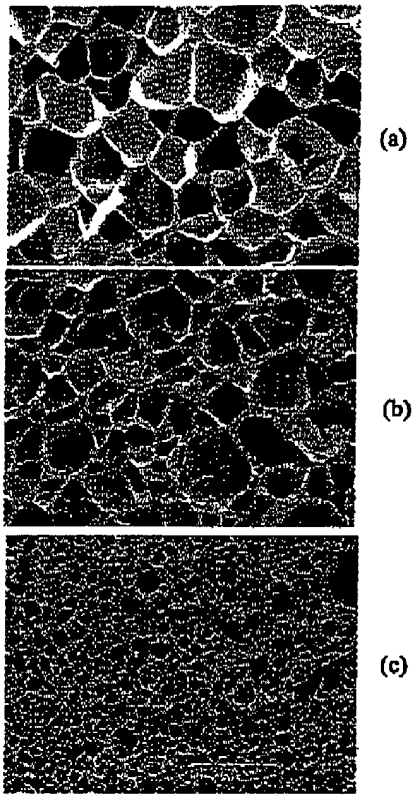

Figure 4 SEM of (a) PMMA; (b) PMMA/5%20A; (c) PMMA/5%MHABS foams. $P(CO_2)=13.79\times10^6$ Pa (2000 psi), T=120°C.

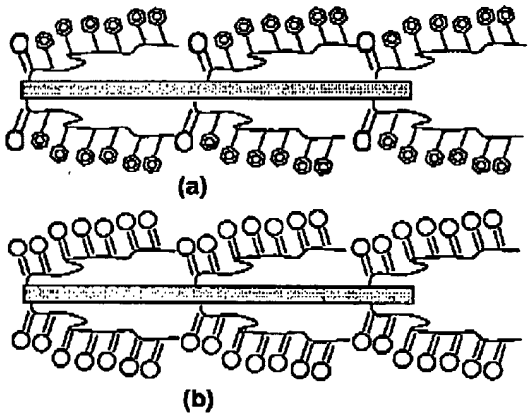

Figure 5 Schematics of copolymers on clay surface in (a) PS/MHABS and (b) PMMA/MHABS nanocomposites.

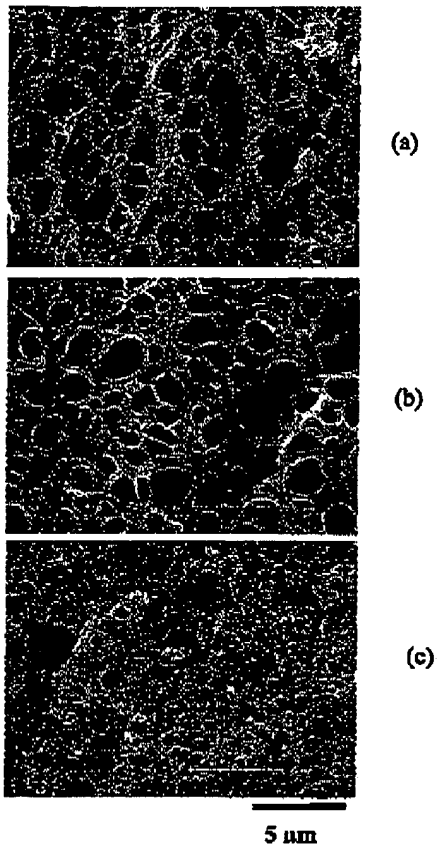

Figure 6 SEM of (a) PMMA; (b) PMMA/5%20A; (c) PMMA/5%MHABS foams by two step foaming.

Figure 7 SEM of foamed region of PLGA nanocomposite scaffold.

EXTRUSION OF POLYSTYRENE FOAMS REINFORCED WITH NANO-CLAYS

Xiangmin Han, Changchun Zeng, Kurt W. Koelling, David L. Tomasko, and L. James Lee
Department of Chemical Engineering, The Ohio State University

Abstract

Nano-clays were used to assist the production of polystyrene microcellular foams. Polystyrene was first compounded with nano-clays and then foamed. The nano-clay was shown to be an effective nucleating agent and caused a reduction in cell size and an increase in cell density. Nanocomposite foams exhibit higher tensile modulus and better fire retardance. The nucleation effect of nano-clay expands the operating windows for extruding microcellular foams. The influence of nano-clays on the sorption of CO_2 and the viscosity of polymer melts are also discussed.

Introduction

Polymeric foams [1-4] are used for many consumer products such as packaging, insulation, cushions, and absorbents due to their light weight, good strength-to-weight ratio, superior insulation abilities, and energy or material absorbing ability. They are also used in some "high-tech" applications such as scaffolds for tissue engineering. Based on the size of fully-grown cells in a cellular polymer, polymeric foams can be classified as macrocellular (>100μm), microcellular (1~100μm), ultra-microcellular (0.1~1μm), and nanocellular (0.1~100nm) foams.

Traditionally, microcellular foams [5,6] are characterized as plastic foams with a cell size smaller than 10 μm and a cell density (cell numbers per unit volume) larger than 10^9 cells/cm^3. This definition is still being debated because it is difficult to relate the properties of polymer foams directly to the cell size and cell density. However, it has been found that microcellular foams can improve some mechanical properties, such as impact strength [7]. Therefore, by applying the technique of microcellular foaming, it becomes possible to produce lightweight polymeric products with high strength.

In this work, nano-sized particles, such as nano-clays, are applied to nucleate micron-sized foams in a continuous extrusion process. Although the heterogeneous nucleation mechanism is still not well understood, it is generally known that the size, shape, and distribution of the particles, as well as the surface treatment can affect the nucleation efficiency.

It has been shown that with the addition of a very small amount of nano-clay into the polymer matrix, the nanocomposites exhibit a substantial increase in many physical properties, including mechanical strength (e.g. tensile modulus and strength, flexural modulus and strength), thermal stability, flame retardance, and barrier resistance [8-13]. Smectite clays, such as montmorillonite (MMT), are of particular interest because they offer a high aspect ratio (100-1000) and a high surface area. Depending on the dispersion of the clay, nanocomposites may possess two idealized structures: intercalated and exfoliated. Intercalation results from limited insertion of polymer chains into the interlayer region and interlayer expansion. Usually the ordered layer structure of the clay is preserved and can be detected by X-ray diffraction. In contrast, extensive polymer penetration and delamination of clay crystallites lead to exfoliated nanocomposites, in which the nanometer-thick silicate platelets are randomly dispersed in the polymer matrix. Exfoliated nanocomposites usually provide the best property enhancements due to the large aspect ratio and large interfacial area between the clay platelets and the polymer.

It is therefore interesting to explore how this difference in particle dispersion affects cell morphology in plastic foams. The addition of nano-clay may benefit both microcellular foam structure and properties. The nano-clay can facilitate the formation of more cells at the same pressure drop and change the cell structure (open or closed) [14, 15]. Nano-clay may also improve the barrier properties (low diffusion coefficient for both mass and heat), mechanical strength, and heat resistance, offering new opportunities for foams in various applications.

In this study, we prepared a series of polystyrene (PS)/clay nanocomposites by extrusion compounding and in-situ polymerization, then used them to prepare nanocomposite foams. The foam structure and properties were characterized. The nucleation effect of the nano-clay was compared with that of talc. Shear viscosity and CO_2 sorption were also studied after the addition of nano-clay.

Experimental

Preparation and Analysis of Nanocomposite Foams

To prepare the intercalated nanocomposites, Cloisite 20A provided by Southern Clay was mechanically blended with a polystyrene resin (AtoFina CX 5197) in a twin-screw extruder. In-situ polymerization was carried out to prepare the exfoliated nanocomposites. As described in our previous work [16], 5 wt.% modified nano-clay, called MHABS, was added to create a fully exfoliated nanocomposite.

The continuous foaming extrusion process was performed on a two-stage single-screw extruder (HAAKE Rheomex 252P). A capillary die with a 0.5 mm diameter and 10 mm long nozzle was custom-made to generate a large and rapid pressure drop. CO_2 was delivered from a

syringe pump (ISCO 260D). CO_2 was compressed to the required pressure in the syringe pump and then injected into the extruder barrel.

Cell size (D_f), which is characterized by the diameter of the foam cells, and cell density (N_f), which is the number of cells per unit volume, are determined by analyzing images obtained from scanning electron micrographs (SEM) using Scion image software.

The foam density was measured by evaluating both the mass and the volume of the sample. The tensile modulus was measured on a Rheometrics Solids Analyzer (RSA II). All samples were short round rods with diameters from 0.5 to 1.5 mm and lengths from 20 to 40 mm. The same pulling speed (0.15 mm/sec) was applied. For comparison, a reduced tensile modulus (i.e., tensile modulus divided by the density of the sample) was calculated to represent the mechanical property. A burning test was also carried out to test the fire resistance.

Shear Viscosity Characterization

The shear viscosity of PS and PS/clay composites without CO_2 was measured at 200°C under the dynamic frequency sweep mode using a Rheometrics Mechanical Spectrometer (RMS 800).

CO_2 Sorption and Desorption

To study the effect of nano-clay on CO_2 solubility and diffusivity, experiments of CO_2 sorption and desorption were performed at low temperatures. The experimental procedure was similar to that employed by Berens et al. [17]. A high-pressure vessel in which flat plate samples of PS or PS/nano-clay composites were loaded was connected to a syringe pump. The samples were saturated with CO_2 at 10 MPa and 50°C for 24 hours. They were then quickly taken out of the high-pressure vessel and placed on a high-resolution balance. The CO_2 desorption curve (weight loss with time) was recorded. From this desorption curve, CO_2 solubility at 50°C was obtained by extrapolating the data back to time zero and CO_2 diffusivity at room temperature was also calculated.

Results and Discussion

Effect of Nano-Clay on Cell Size

Each montmorillonite clay particle contains thousands of individual layers with a thickness dimension of ~1 nm and a lateral dimension of ~1000 nm. To take advantage of its high aspect ratio (100-1000) and large surface area, the layers should be separated as far as possible. This in turn provides more nucleation sites.

PS and PS/5% 20A intercalated nanocomposites were foamed at different pressure drops by changing the screw rotation speed (10 to 30 rpms). The foaming temperature was the same (200°C) and the CO_2 concentration was kept at 4 wt.%. The exfoliated PS/5% MHABS was only foamed at one screw rotation speed (10 rpm) for two foaming temperatures (200°C and 240°C) due to the limited amount of material available.

The results are summarized in Figure 1, which exhibits how cell size and cell density change as the pressure drop rate increases. An interesting observation is that the decrease in cell size slows at high pressure drop rates, while the cell density increases nearly linearly. The cell size of nanocomposites is smaller than 10 μm and the cell density is larger than 10^9 cells/cm^3 when the pressure drop rate is greater than 10^9 Pa/sec. At a screw rotation speed of 10 rpm, the exfoliated nanocomposite creates the smallest cells and the largest cell density. Conversely, no pure PS foam has a cell density higher than 10^9 cells/cm^3 at these operating conditions, although cell sizes smaller than 10 μm can be obtained.

Compared with pure PS, nanocomposites broaden the operating windows for making microcellular foams. To achieve the same cell size and cell density, nanocomposites require lower pressure drop rates, which means a larger die opening can be used at the same flow rate. The foaming temperature applied in this study is much higher than the T_g of PS (~ 105°C). With a decrease of the foaming temperature, a higher pressure drop rate can be obtained due to the increased melt viscosity. As a result, a smaller cell size and higher cell density may be achievable. Experiments to validate these hypotheses are being conducted in our lab.

Shear Viscosity of PS Nanocomposites

In the extrusion foaming process, viscosity is an important parameter that determines the pressure profile and cell growth. Shear viscosities of non-foamed PS and PS/clay nanocomposites were measured at 200°C under the dynamic frequency sweep mode by using the Rheometrics Mechanical Spectrometer (RMS 800). As shown in Figure 2, the addition of the clay increases the shear viscosity of the polymer melt. The more clay added, the higher the viscosity. The exfoliated nanocomposite shows the highest shear viscosity. With the same flow rate and same dimension of the extrusion die, a higher shear viscosity can create a larger pressure drop rate that benefits the formation of more nucleation sites.

The effect of CO_2 on the shear viscosity of PS nanocomposites is the subject of another paper in this conference.

CO_2 Sorption and Desorption

Figure 3 shows desorption curves of three samples, PS, PS/5% 20A, and PS/5% MHABS. By extrapolating the desorption data back to time zero, the solubility of CO_2 in PS, PS/5% 20A, and PS/5% MHABS at 50°C and 10 MPa was found to be 8.5, 8.5, and 8.8 wt.%, respectively. Carbon dioxide exhibits a slightly higher solubility in the exfoliated PS nanocomposite. Additionally, the diffusivity at room temperature was calculated based on the three desorption curves by assuming a one-dimensional diffusion. The results are

4.5×10^{-7}, 3.1×10^{-7}, and 3.2×10^{-7} cm^2/sec for PS, PS/5% 20A, and PS/5% MHABS. Obviously, the addition of nano-clay can slow down the CO_2 diffusion out of the sample.

Comparison between Talc and Nano-Clay as a Nucleating Agent

Talc, non-aluminous magnesium silicate hydroxide ($Mg_3Si_4O_{10}(OH)_2$), is a very common nucleating agent in the foaming industry. The nucleation effect of nano-clay was compared with that of talc. SEM micrographs of cell structure with different nucleating agents are shown in Figure 4. Obviously, nano-clay is most effective for reducing the cell size and increasing the cell density.

Figure 4 also shows the SEM micrographs at high magnifications for both the intercalated PS/5% 20A nanocomposite foam and the exfoliated PS/5% MHABS nanocomposite foam. For the intercalated nanocomposite foam, cells smaller than 500 nm are found to nucleate and grow around clay tactoids, while in the exfoliated nanocomposite foam, much finer structures can be observed on the cell wall (although it is hard to tell whether these structures are tiny cells or only the surface roughness). In the intercalated case, cells are stretched like a cigar according to the particle shape, because of the large aspect ratio of the nano-clay particle.

Tensile Modulus and Burning Test

The tensile modulus was measured on a Rheometrics Solids Analyzer (RSA II). For comparison, a reduced tensile modulus (i.e., tensile modulus divided by the density of the sample) is calculated to represent the mechanical property. As shown in Figure 5, the nanocomposite foams exhibit a higher reduced modulus, although the modulus is still lower than that of non-foamed pure PS. Compared to the non-foamed PS sample, the exfoliated nanocomposite foam sample has about 31% weight reduction with a sacrifice in the reduced modulus of about 19% from 2.6 to 2.1 $GPa/g/cm^3$. In comparison, the PS/talc foam has about 29% weight reduction and a decrease of 43% in reduced modulus.

Nanocomposite foams also show enhanced fire retardance. A simple burning test was performed as shown in Figure 6. A piece of soft paper soaked with ethanol was placed on the table and the foam samples were ignited and burned above it. For the pure PS foam (Figure 6a), the burning sample dripped down quickly and ignited the paper. On the contrary, the nanocomposite foam sample (PS/5%20A) forms a char during burning without dripping, thus preventing the fire from spreading (Figure 6b).

Conclusions

Intercalated and exfoliated PS nanocomposites were synthesized and continuous extrusion foaming was conducted to prepare nanocomposite foams. Nano-clay shows a higher nucleation efficiency than talc. At a screw rotation speed of 10 rpm and a die temperature of 200°C, the addition of a small amount (i.e., 5 wt.%) of intercalated nano-clay greatly reduces cell size from 25.3 to 11.1 μm and increases cell density from 2.7×10^7 to 2.8×10^8 $cells/cm^3$. Once exfoliated, the nanocomposite exhibits the highest cell density (1.5×10^9 $cells/cm^3$) and smallest cell size (4.9 μm) at the same particle concentration.

The addition of nano-clay was found to increase the shear viscosity of polymer melts and slow down the CO_2 diffusion.

Compared with pure polystyrene foams, polystyrene nanocomposite foams can provide superior performance, including higher tensile modulus, better surface quality, and enhanced fire retardance.

Acknowledgments

The authors would like to acknowledge financial support from the National Science Foundation (DMI-9908289) and the Center for Advanced Polymer and Composite Engineering at The Ohio State University. The materials were donated by Southern Clay and Owens Corning.

References

1. Klempner, D. and Frisch, K. C., eds. *Handbook of Polymeric Foams and Foam Technology*. . 1991, Oxford University Press: Munich; Vienna; New York.
2. Landrock, A. H., *Handbook of Plastic Foams: Types, Properties, Manufacture and Applications*. 1995, Miller Road, Park Ridge, New Jersey: Noyes Publications.
3. Khemani, K. C., *Polymeric Foams: Science and Technology*. 1997: ACS Symposium Series.
4. Lee, S.-T., *Foam Extrusion: Principles and Practice*. 2000, Lancaster, PA: Technomic Publishing Company, Inc.
5. Martini-Vvedensky, J. E., Suh, N. P., and Waldman, F. A., *Microcellular closed cell foams and their method of manufacture*, US 4,473,665 (1984)
6. Park, C. B., Suh, N. P., and Baldwin, D. F., *Method for Providing Continuous Processing of Microcellular and Supermicrocellular Foamed Materials*, US 5,866,053 (1999).
7. Kumar, V. and Weller, J. E., *Microcellular Foams*, in *Polymeric Foams: Science and Technology*, K.C. Khemani, Editor. 1997. p. 101.
8. Lan, T., Kaviratna, P. D., and Pinnavaia, T., *J. Chem. Mater.*, 6 573 (1994).
9. Okada, A. and Usuki, A., *Mater. Sci. Eng.*, C3 109 (1995).
10. Kojima, Y., Usuki, A., Kawasumi, M., Okada, A., Fukushima, Y., Kurauchi, T., and Kamigaito, O., *J. Mater. Res.*, 8 1185 (1993).

11. Zeng, C. and Lee, L. J., *Macromolecules*, 34 4098 (2001).
12. Wang, H., Zeng, C., Elkovitch, M., Lee, L. J., and Koelling, K. W., *Polymer Engineering and Science*, 41 (11), 2036 (2001).
13. Svoboda, P., Zeng, C., Wang, H., Lee, L. J., and Tomasko, D. L., *Journal of Applied Polymer Science*, 85 (7), 1562 (2002).
14. Han, X., Zeng, C., Lee, L. J., Koelling, K. W., and Tomasko, D. L., *SPE-ANTEC*, 1915 (2002).
15. Zeng, C., Han, X., Lee, L. J., Koelling, K. W., and Tomasko, D. L., *SPE-ANTEC*, 1504 (2002).
16. Zeng, C. and Lee, L. J., *SPE-ANTEC*, 2213 (2001).
17. Berens, A. R., Huvard, G. S., Korsmeyer, R. W., and Kung, F. W., *J. Appl. Polym. Sci.*, 46 (2), 231 (1992).

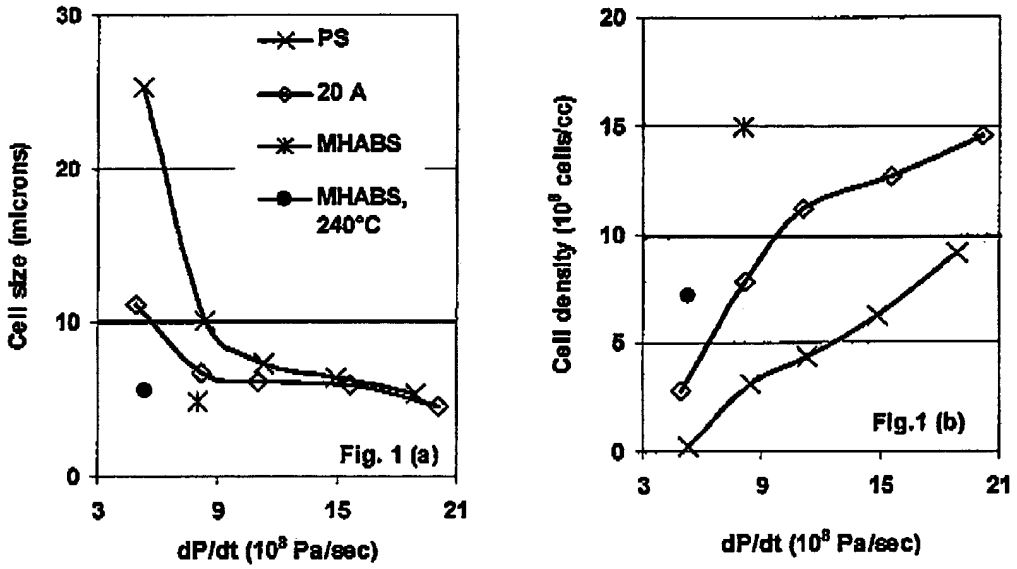

Figure 1. Cell size (left) and cell density (right) of PS and PS nanocomposites at different pressure drop rates (one data point of MHABS is at 240°C, and all others are at 200°C).

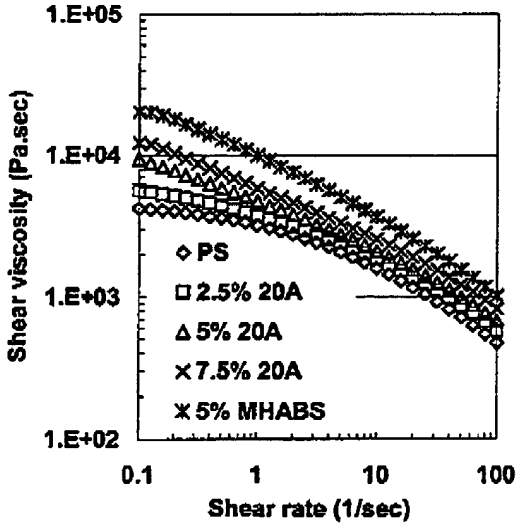

Figure 2. Effect of nano-clay on shear viscosity.

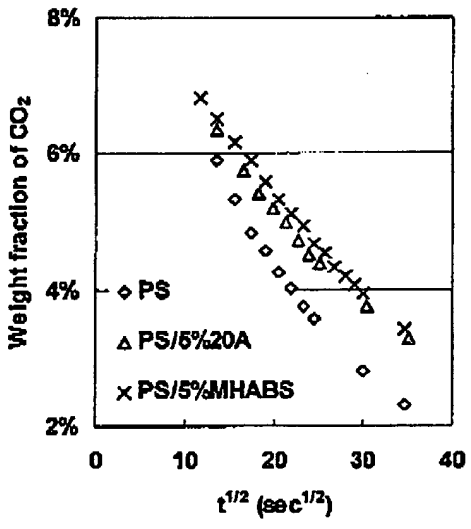

Figure 3. CO_2 desorption from PS and PS nanocomposites.

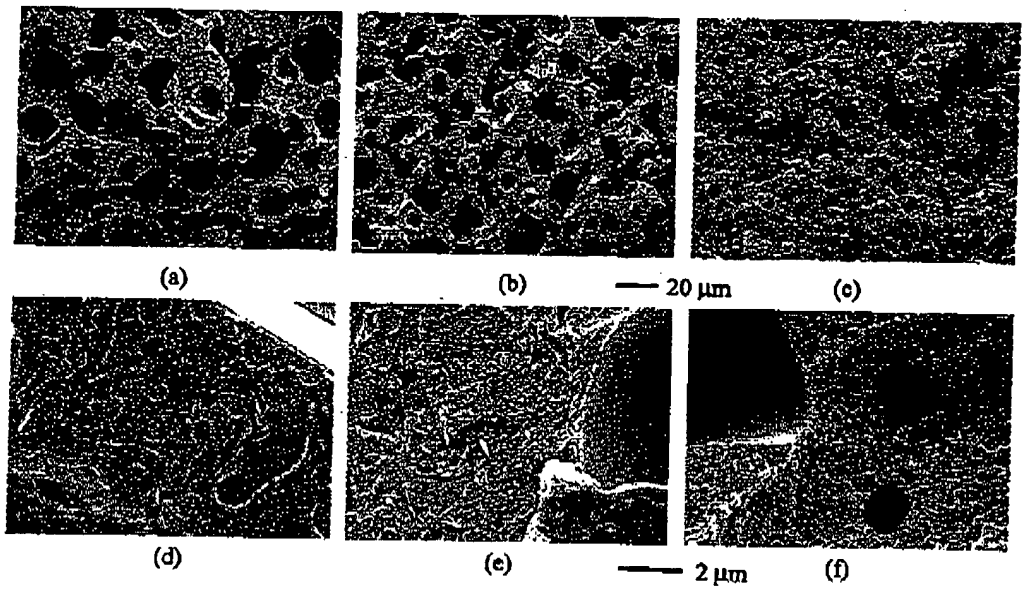

Figure 4. Comparison of talc and nano-clay as the nucleating agent at 200°C ((a) and (d): 5% talc; (b) and (e): 5% 20A; (c) and (f): 5% MHABS).

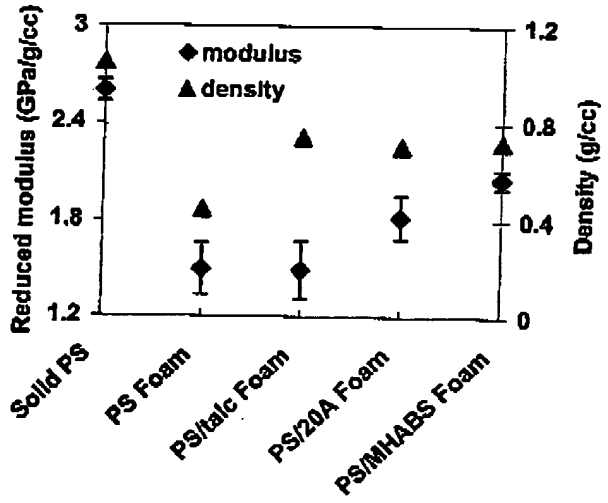

Figure 5. Reduced tensile modulus of different foamed samples.

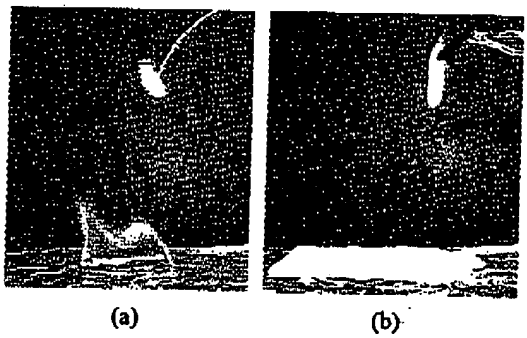

Figure 6. Burning test of (a) PS foam sample, and (b) PS/5 wt.% 20A nanocomposite foam sample.